Entry-level spin distributions and relative γ-neutron branching ratios of samarium isotopes populated by the (p,t) reaction

N. Cooper, C. W. Beausang, P. Humby, A. Simon, J. T. Burke, R. O. Hughes, S. Ota, C. Reingold, A. Saastamoinen, and E. Wilson

Phys. Rev. C **98**, 044618 — Published 24 October 2018

DOI: 10.1103/PhysRevC.98.044618

Entry-Level Spin Distributions and Relative γ-Neutron Branching Ratios of Samarium Isotopes Populated by the (p,t) Reaction

N. Cooper,[1,2] C. W. Beausang,[2,*] P. Humby,[2,3] A. Simon,[1] J. T. Burke,[4] R. O. Hughes,[4] S. Ota,[4] C. Reingold,[1] A. Saastamoinen,[5] and E. Wilson[2]

[1] *Department of Physics and the Joint Institute for Nuclear Astrophysics, University of Notre Dame, Notre Dame, Indiana 46556, USA*
[2] *Department of Physics, University of Richmond, Richmond, Virginia 23173, USA*
[3] *Department of Physics, University of Surrey, Guildford, GU2 7XH, UK*
[4] *Nuclear and Chemical Sciences Division, Lawrence Livermore National Laboratory, Livermore, California 94550, USA*
[5] *Cyclotron Institute, Texas A&M University, College Station, Texas 77843, USA*

The spin distribution populated in ^{150}Sm(p,t) reaction with 25 MeV protons has been investigated using the silicon telescope and high-purity germanium array Hyperion. Angular distributions of outgoing tritons and relative intensities of γ rays from low-lying levels are used to deduce the initial spin distribution using statistical calculations and are compared with a semi-classical model of the (p,t) reaction. Experimental and theoretical results suggest a peak strength near $4\hbar$ when gated on outgoing tritons detected in Hyperion, while the full 4π distribution may peak near $2\hbar$. Additionally, the average γ-neutron branching ratio is determined from the data with the aid of one of two new codes presented in this work. The analysis is extended to other recent studies of ^{152,154}Sm(p,t) to form systematics of the spin-dependence of the surrogate method applied to heavy nuclei in the transitional to deformed region.

PACS numbers: 24.87.+y,21.10.Hw, 24.30.Cz

I. INTRODUCTION

Measurement of reaction cross sections, such as (n,γ) and (n,f), away from stability are often difficult or infeasible due to the short lifetime of required target or projectile nuclei. These cross sections are an essential input in calculations of astrophysical interest as well as reactor design and stockpile stewardship. In many cases, these reaction cross sections cannot be measured directly, so indirect methods must be employed. One such method for determining the partial cross sections of a particular reaction channel is the surrogate method. A central assumption of the method is that the direct and surrogate reaction exit through the same channel. This follows from the idea of the compound nucleus, first introduced by Bohr. The cross section for formation of the compound nucleus during the reaction can typically be calculated accurately using optical models; however, the decay rates via different channels often have large uncertainty and must be measured to determine accurate partial cross sections.

While the surrogate method dates back to the 1970s [1], there has been a recent resurgence in the interest and use following the development of next-generation radiation detection equipment and large detector arrays, allowing further scrutiny into the viability of the method. In particular, differences in the spin distribution populated by the surrogate reaction influence the results of certain approaches to the method. It is observed that deduced γ-neutron branching ratios above the neutron separation energy depend on the detection angle relative to the beam axis as well as placing a constraint on spin by requiring a coincident γ-ray emission from yrast levels of a specific spin [2]. This is due to the fact that the levels of a given spin tend to decay though a cascade of levels of a similar spin on the yrast band by dipole transitions which dominate and increase in strength with energy below the giant dipole resonance energy. The surrogate method is often applied in the Weisskopf-Ewing limit of Hauser-Feshbach theory, in which the branching ratio for a particular decay is assumed to be independent of the spin and parity of the entry level. There have been recent efforts to examine the effects of the differences in spin distributions as it relates to the method [3], of which the current work is a part.

In this paper, results from an experiment using the recently commissioned Hyperion array, located at the Texas A&M Cyclotron institute, are presented. These results, along with those from past experiments on Samarium isotopes [4], are used to extract the spin distribution of the intended surrogate reaction using theoretical models of γ-ray emission and compared with a semi-classical calculation of the spin distribution resulting from light-ion, heavy-target reactions. Two new codes, not previously presented in literature, will be discussed, as well as conclusions and outlook of the results.

II. THE SURROGATE METHOD

The total cross section for the decay of a nucleus through a channel χ following a reaction in which the compound nucleus b is formed with excitation energy E_x may be expressed as a function of spin and parity as

* Deceased June 3 2017.

$$\sigma_{b\chi}^{\rm CN}(E_x) = \sum_{J,\pi} \sigma_b^{\rm CN}(E_x, J, \pi) G_\chi(E_x, J, \pi), \qquad (1)$$

where G_χ is the branching ratio for the decay mode χ, and $\sigma_b^{\rm CN}$ is the cross section for formation of the compound nucleus of a specific spin and parity. In the Weisskopf-Ewing limit, the G_χ are independent of J and π, and thus the total cross section for the reaction channel may be written as

$$\sigma_{b\chi}^{\rm CN}(E_x) = \sigma_b^{\rm CN}(E_x) G_\chi(E_x). \qquad (2)$$

An experimentally measurable quantity is given by the probability of a given decay channel χ for a given compound nucleus formation b, given by

$$P_{b\chi}(E_x) = \frac{N_{b\chi}(E_x)}{N_b(E_x)}, \qquad (3)$$

where N_b and $N_b\chi$ are the number of efficiency-corrected total and coincident events, respectively. This may also be written in the form

$$P_{b\chi}(E_x) = \sum_{J,\pi} F_b^{\rm CN}(E_x, J, \pi) G_\chi(E_x, J, \pi), \qquad (4)$$

where $F_b^{\rm CN}$ is the probability distribution of populating a nucleus in a level of given excitation energy, spin, and parity. In general, values of this function obtained from the surrogate reaction will differ from those of the desired reaction, and will be specific to the experimental data due to constraints such as detector solid angle. Under the assumption of the Weisskopf-Ewing limit, Eq. (4) simplifies to

$$P_{b\chi}(E_x) = G_\chi(E_x). \qquad (5)$$

When using the so-called ratio surrogate method [5], this simplifies the measurement of pairs of nuclei a and b to

$$\frac{\sigma_{a\chi}}{\sigma_{b\chi}} = \frac{\sigma_a^{\rm CN} N_{b\chi}}{\sigma_b^{\rm CN} N_{a\chi}}, \qquad (6)$$

under the assumption that the formation and subsequent-decay cross sections are approximately equal, and that the density of the target and number of total projectiles are equal. Discrepancies due to experimental conditions may be measured and used to correct for differences in the latter two conditions.

Recent works utilizing the surrogate method have produced results with various degrees of agreement with known cross sections measured directly, and the dependence of branching ratios on spin has been emphasized in recent works [2, 3, 6]. Thus a method of correcting for the differences due to spin distribution of the reactions is of paramount importance to the application of the method, as the difference between results produced under the assumptions exhibited by Eqs. (1) and (2) may have a significant impact on resulting cross sections extracted from experiment and theory. Recent investigations have used the methods of fitting calculations using the Distorted Wave Born Approximation [7] and by gating on individual low-lying γ rays in a particle-γ coincidence in order to dertermine the spin distribution and dependence of the branching ratio.

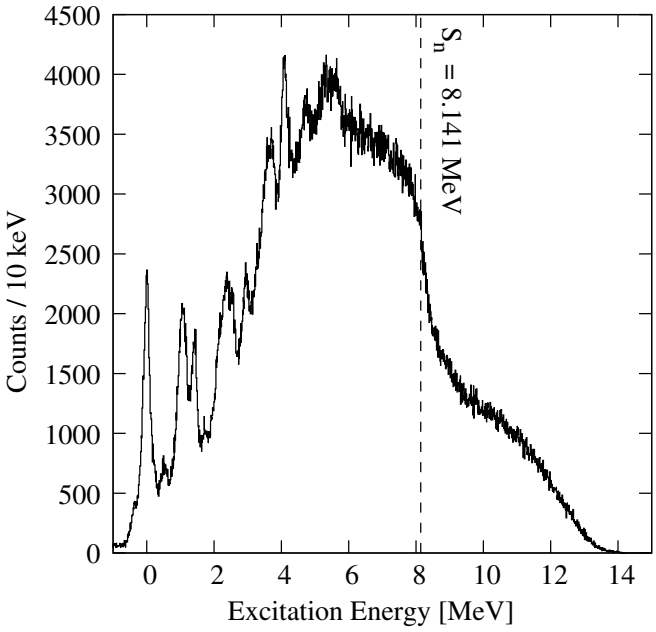

FIG. 1. Excitation-energy spectrum of ^{148}Sm in the ^{150}Sm(p,t) channel, obtained by triggering on triton in the silicon telescope and performing kinematic corrections to the particle energy.

III. EXPERIMENTAL DETAILS

An experiment was performed at the Texas A&M cyclotron institute utilizing 25 MeV protons accelerated by the K150 cyclotron. The protons were incident on a 1 mg/cm^2 foil of approximately 98% enriched ^{150,152,154}Sm targets. Outgoing particles were detected by the Silicon Telescope for Reaction Studies (STARS) [8], while γ rays were detected by a high-purity germanium clover array consisting of 13 detectors from the former Livermore, Texas, Richmond (LiTeR) [9] and the Clovershare collaboration. The clover manifold is designed to hold detectors in three planes, one in the plane of the beam axis and the horizontal, and the other two at upward and downward angles of 45°. Six detectors were placed in the beam-horizontal plane, while the other seven were placed at 45° relative to horizontal detectors, with the exception of the lower detector facing upstream being absent. STARS resides within the target chamber and consists of two thin, nearly cylindrical silicon detectors, and the present experiment combined detectors of thickness 50 μm for the ΔE with a 1.5 mm $E1$ detector, detecting deuterons and protons beyond the summed

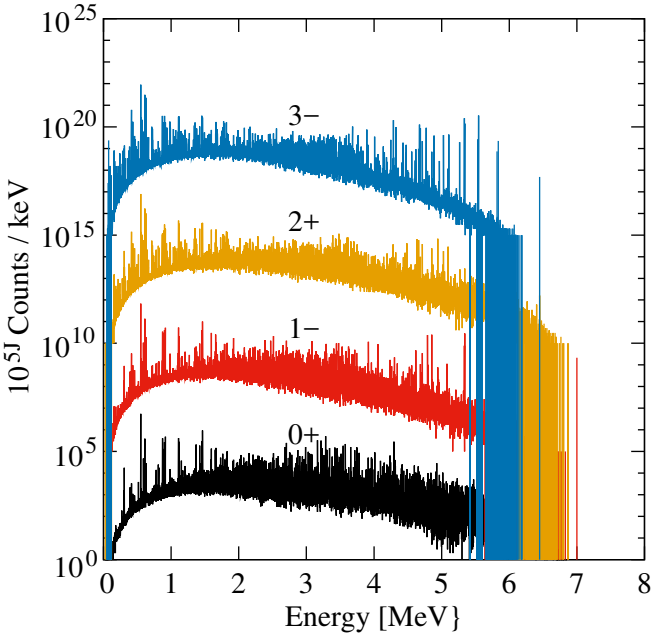

FIG. 2. (Color online) Simulated γ-ray spectra from natural parity levels of ^{148}Sm at 7 MeV using MCγ for a single nuclear realization. Note that the spectra have been scaled by 10^{5J} for visibility, and with exception of primary γ-rays, the intensity decays to negligible values above approximately 5 MeV.

beam energy and Q values. Both detectors are segmented into 24 rings and 8 segments for angular resolution. The collective detector array, Hyperion [10], which includes a newly-designed target chamber and HPGe clover manifold, collected data using a ΔE-E1 trigger. An example spectrum of reconstructed excitation energy of the residual nucleus of ^{150}Sm(p,t) is presented in Fig. 1. The resolution of excitation energy was approximately 130 keV, while that of the clover γ-ray energy was approximately 0.5%.

IV. MODELING OF γ-RAY EMISSION

A so-called statistical model of γ-ray emission is often used to produce γ-ray spectra following nuclear reactions. The model assumes mean values defined by γ-ray strength functions and level density, as well as distributions for both as a function of the mean value. These distributions are given by the Porter-Thomas distribution of partial decay widths [11] and Wigner distribution, both of which originate from the theory of random matrices with Gaussian matrix elements. These distributions have also become associated with the phenomenon of quantum chaos [12].

The Fortran code DICEBOX [13] is widely used for γ-ray-emission calculations invoking such models. Another code, MCγ [14] (referred to as Cascade in the reference), has also been developed in Java using an identical algorithm. Total and primary γ-ray spectra show good agreement with those of DICEBOX projected from the matrix presented as supplementary material in Ref. [15], and are presented in Fig. 4.2 of Ref. [14]. Randomly generated nuclei with properties which should be consistent with experimental data and/or models, called *realizations* in many works, are created by first randomly generating levels using a Wigner distribution with a mean specified by the level density. For each level, a random seed of the random number generator is stored, along with other properties of the level, such as spin, parity, and energy. The seed is then subsequently called in order to produce consistent γ-ray transition widths for each randomly generated level during the simulation. Transition widths between levels are then randomly evaluated using a specified strength function and the Porter-Thomas distribution, equivalent to a χ^2 distribution with one degree of freedom and with a mean determined by the strength function. For the present work on ^{148,150,152}Sm γ-ray cascades, parameters of the backshifted-Fermi gas model obtained from experimental fits were taken from Refs. [16, 17], and for the current work, standard Lorentzian giant dipole resonance parameters were taken from the RIPL-3 compilation [18].

Total γ-ray energy spectra produced by MCγ for natural parity levels at 7 MeV of ^{148}Sm are presented in Fig 2. The spectra exhibit differences in intensity as a function of spin, and thus the intensities of known γ rays provide information characteristic of the spin distribution populated by a particular reaction. This is due to the fact that nuclei have the tendency to populate the yrast band by decay through relatively few strong dipole transitions, and thus do not change in spin significantly between the entry level and the yrast band. The intensities from these spectra are used for comparison to the data and extraction of the spin distribution populated.

V. MODELING OF (p,t)

The (p,t) reaction was modeled in the current work using semi-classical methods and implemented within a new code called PTCruiser. The quantum-mechanical aspect of the model is the assumption that the momentum distribution of nucleons in the target nucleus is that of an ideal Fermi gas at zero temperature. Inelastic collisions between the proton beam and neutrons within the nucleus are simulated under the assumption that the mean free path of protons and deuterons passing through the nucleus is large compared to the size of the nucleus. This assumption implies that interaction between the incident protons is uniformly distributed over the nuclear volume. The probability of interaction between the incident protons and neutrons within the nucleus is proportional to the density of neutrons, which is taken to be the form of a Woods-Saxon potential, given by

$$\rho_\nu(\vec{r}) = \frac{\rho_{0\nu}}{1+\exp\left(\left|\vec{r}-\vec{R}(\beta,\theta,\phi)\right|/a\right)}, \qquad (7)$$

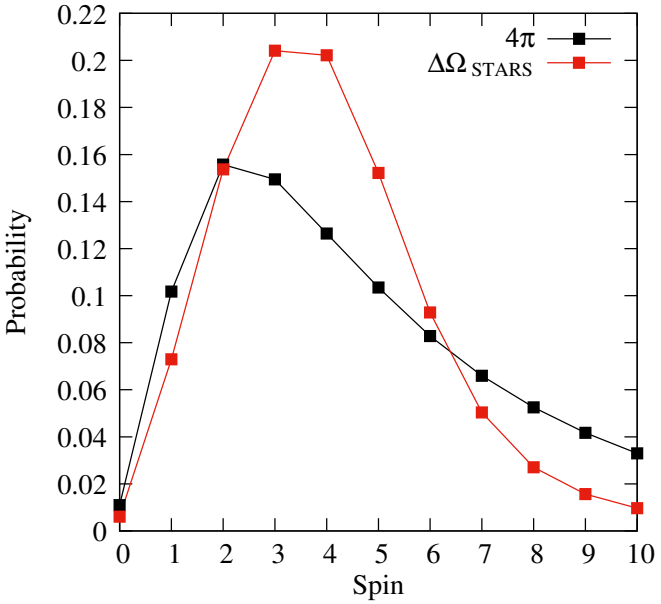

FIG. 3. (Color online) Probability densities calculated by PTCruiser of entry-level spin for ^{150}Sm(p,t) between 2.5 MeV and 7.5 MeV excitation energy for a 4π detector and that of STARS in the present experiment, spanning the angles of 27.5° to 54°.

where $\rho_{0\nu}$ is the density of neutrons at $r = 0$, β is the quadrupole deformation parameter, θ and ϕ describe the orientation of the nucleus relative to the beam axis, and a is the diffuseness of the nuclear surface. The parameters β were taken from Ref. [19], while the θ and ϕ were randomized during the calculation. The incident proton beam is assumed to be approximately twice as large as the mean nuclear radius, as the outgoing tritons are assumed to be produced within a single nucleus as is required to produce the nucleus of interest. A calculation for the present experiment of ^{150}Sm(p,t) is shown in Fig. 3. The difference in the probability distributions results from a truncated spin transfer to the nucleus when detected at the solid angle spanned by the STARS detector.

VI. SPIN DISTRIBUTIONS AND γ-RAY INTENSITIES

Intensities of yrast γ rays were obtained from the present experiment by gating on 1 MeV intervals centered around excitation energies of 3, 5, and 9 MeV of ^{148}Sm populated in ^{150}Sm(p,t). A comparison of a combined calculation of MCγ and PTCruiser with this data is shown in Fig. 4. The same comparison for ^{152}Sm(p,t) and ^{154}Sm(p,t) is shown in Figs. 5 and 6, respectively. Matrices of γ ray intensity versus natural spin-parity were produced using MCγ, and used to extract the spin distribution using the equation

$$I_i = \sum_j M_i^j F^j, \tag{8}$$

where F is the spin distribution of Eq. (4), M is the matrix of intensity from the most intense γ rays from the yrast levels produced as a function of spin by calculation with MCγ, and I is the experimental γ-ray intensity vector. The indicies i and j enumerate the γ-ray transition and spin of the entry level, respectively. A standard Lorentzian photon strength function for both $E1$ and $M1$ decays and back-shifted Fermi gas level density model were assumed for the calculation. While a natural cutoff is provided by the spin distribution of the level density and far lower strength of high-multipolarity transitions, only dipole transitions were used in the current work as uncertainties in the strength function for higher multipolarity transitions are large, as is clear from Ref. [18]. The fit of F to the data was performed using random simulation of the distribution F between spins zero and 10 using Eq. (8), under the conditions that the elements are positive and sum to unity. A probability vector spanning the region of zero to 10 was fitted to the data using χ^2 minimization. Resulting fits are presented in Fig. 7 along with calculations from PTCruiser produced with excitation energy and angle gates of the respective experiment.

The agreement between experimental γ-ray intensities and theory for ^{154}Sm(p,t) exhibited in Fig. 4 as well as for the spin distributions extracted and presented in Fig. 7 bodes well for the theoretical models presented. Intensities at higher energies observed from ^{152}Sm(p,t) and ^{154}Sm(p,t) in Figs. 5 and 6 likewise agree around 7 MeV, but exhibit poorer agreement at lower energies. This may be because the type of statistical model of γ-ray emission used in this work is generally used to describe regions of high level density where the nuclear properties have been suggested to exhibit the chaotic properties previously mentioned, such as heavy nuclei or highly-excited nuclei. The level of agreement produced here affirms that expectation. However, one source of uncertainty in this conclusion lies in the fact that ^{152}Sm is a daughter nucleus of ^{152}Eu, which is commonly used (as in this work and separately in the others) as an efficiency calibration source. Thus, one would expect relative intensities of known levels required by MCγ and to produce the theoretical spin distribution to be more accurate for ^{154}Sm(p,t). Another possible contribution to the differing level of agreement is the transition from spherical to deformed nuclei, where the level density rapidly increases, occurs near ^{152}Sm on the isotopic chain. Considering these two possible effects, it is unclear whether the staggering of the spin distribution extracted from the experimental data using MCγ of ^{150,152}Sm(p,t), as opposed to that of ^{154}Sm(p,t), is a nuclear structure effect. However, as the efficiency of the array should have been well-determined during the experiments, it is suspected that the staggering is a structure effect. Conclusively determining the exact origin the spin staggering effect may be aided by recent data taken by

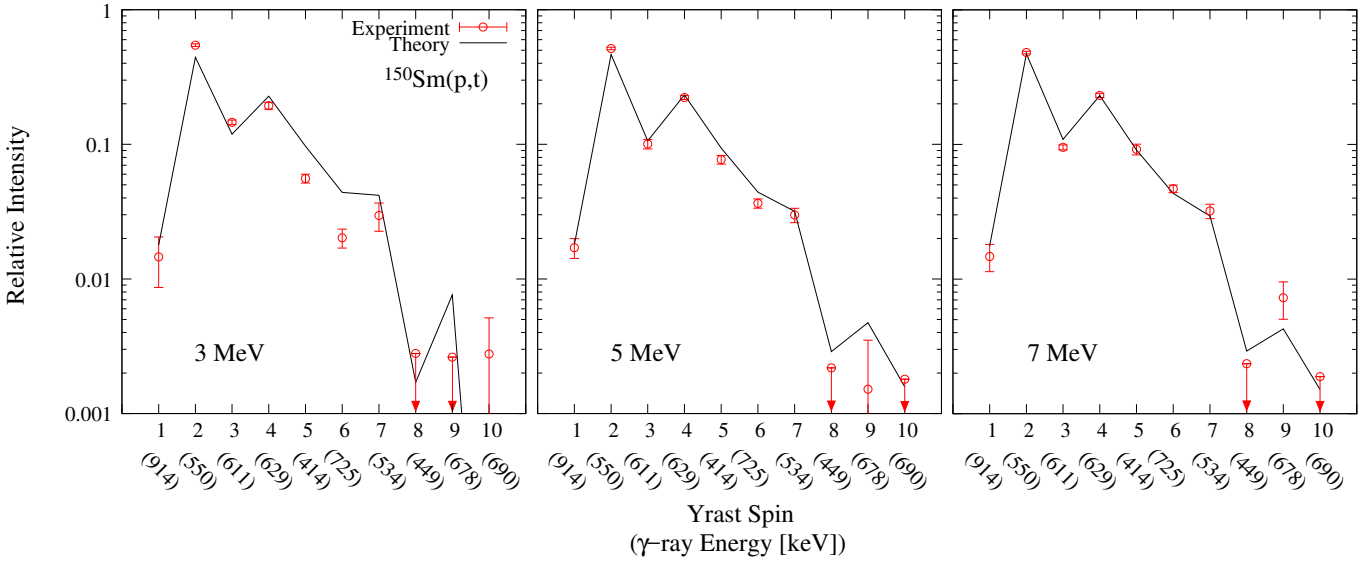

FIG. 4. (Color online) Experimental relative intensities of the most intense γ rays from yrast levels of ^{148}Sm following the ^{150}Sm(p,t) reaction at 25 MeV proton energy (red points) and theoretical intensities of combined calculations from MCγ and PTCruiser. Both the experimental and calculated intensities are normalized to sum to unity.

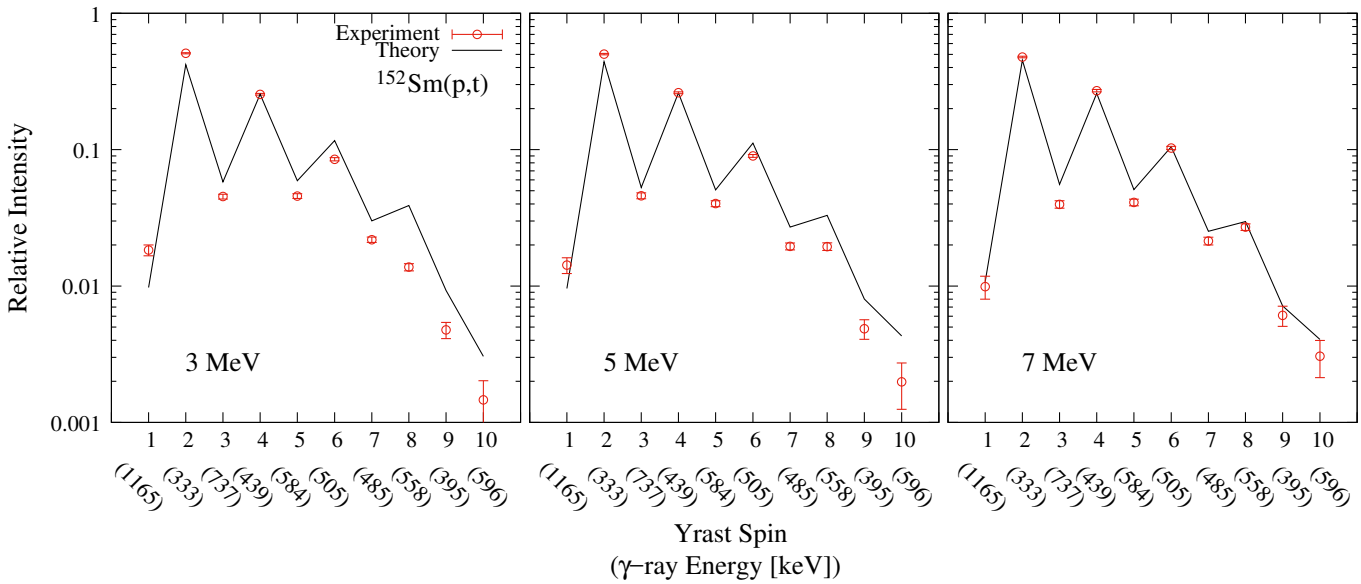

FIG. 5. (Color online) Same as in Fig. 4, except for ^{152}Sm(p,t).

Hyperion as well as future experiments.

The approximate independence of spin on energy calculated by PTCruiser and extracted from the presented experimental data supports the further use and investigation of the Oslo method [20] used to extract γ ray strength functions and level densities, a method which assumes spin independence of the reaction on the excitation energy of the product nucleus. Work utilizing the Oslo method, which is concurrently being performed on the Hyperion experimental data, may benefit from analysis presented in this work.

VII. BRANCHING RATIOS ABOVE THE NEUTRON SEPARATION ENERGY

Using the data from the experiments presented, it is possible to determine the average γ-total branching ratio $\langle\Gamma_\gamma/\Gamma_T\rangle$, where Γ_γ and Γ_T are the γ-ray-emission width and the total decay width of the individual levels populated, respectively. Above the neutron separation energy, a fit to the γ intensity using the same methods used to determine the spin below yields a vector proportional to the product of spin probability and γ-neutron branching ratio. Under the assumption that we may accurately cal-

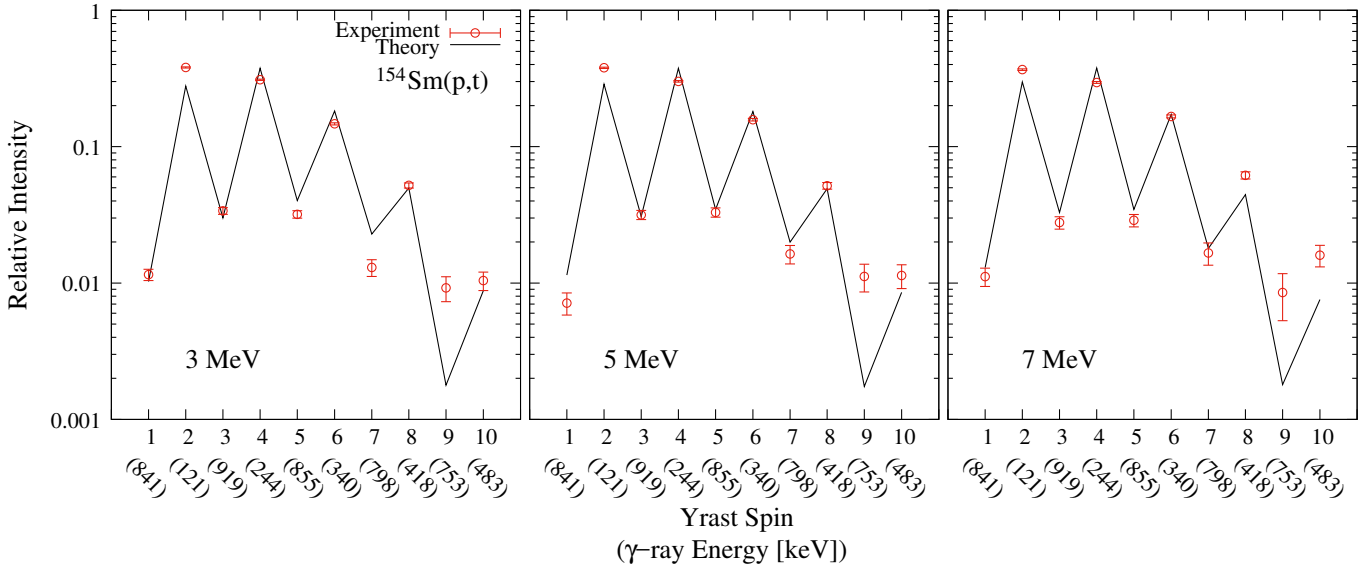

FIG. 6. (Color online) Same as in Fig. 4, except for ^{154}Sm(p,t).

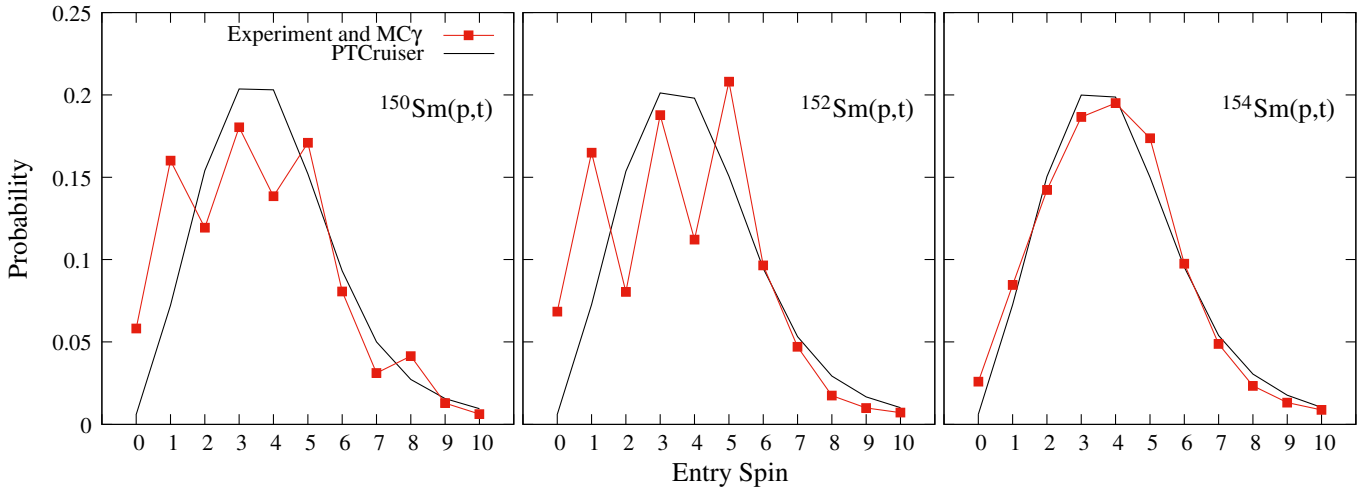

FIG. 7. (Color online) Spin distributions deduced using MCγ and experimental data from Hyperion and STAR-LiTeR in the Sm(p,t) channel with 25 MeV protons compared with results from PTCruiser. The experimental excitation energy range gated on in the calculation is between 2.5 MeV and 7.5 MeV, using only outgoing tritons detected between 27.5° and 54° for the current work with Hyperion, and 34° and 58° for the STAR-LiTeR experiments. The method for extracting the spin distribution from the experimental data is described in the text.

culate or experimentally determine the spin distribution, this leads to a method to determine $\langle\Gamma_\gamma/\Gamma_T\rangle$ by division of the two distributions. This is due to the fact, that above the neutron separation energy, Eq. (8) becomes

$$I_i = \sum_j M_i^j F^j \langle\Gamma_\gamma/\Gamma_T\rangle^j \,, \tag{9}$$

and thus inversion of the matrix M and division by individual elements of F gives $\langle\Gamma_\gamma/\Gamma_T\rangle$. Results from the present experiment produced using the data below and above the neutron separation energy to extract I, as well as MCγ to produce the matrix M, are shown in Fig. 8. The origin of the large values of $\langle\Gamma_\gamma/\Gamma_T\rangle$ as zero and 10 are approached may be due to slightly differing spin distributions below and above the neutron separation energy. This form of the resulting spin distributions indicates that the width of the distribution may increase as a function of energy, leading to the apparent rise in the branching ratio at the endpoints of the distribution. The relatively constant ratios extracted for the most intensely-populated levels indicates that use of the Weisskopf-Ewing limit may be a good approximation, although the staggering which appears to be present in the lesser-deformed Samarium isotopes indicates a possible need to introduce corrections into the theory of surrogate reactions beyond the Weisskopf-Ewing limit.

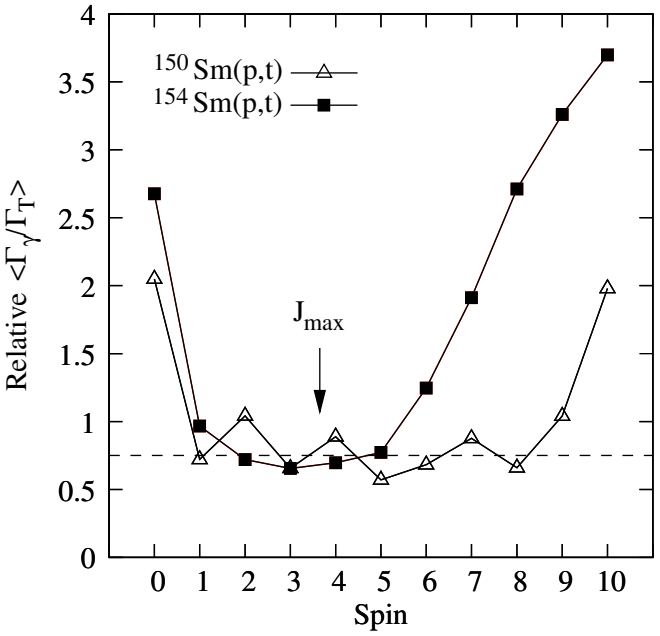

FIG. 8. Relative average branching ratios $\langle\Gamma_\gamma/\Gamma_T\rangle$ above the nuetron separation energy produced by experimental data and MCγ for ^{150}Sm(p,t) and ^{154}Sm(p,t). The arrow indicates the peak intensity as a function of spin populated by the experiment, while the dashed line illustrates a constant ratio expected from the Weisskopf-Ewing limit.

VIII. SUMMARY AND OUTLOOK

Results have been presented from the ^{150,152,154}Sm(p,t) reactions using data taken by Hyperion (previously STAR-LiTeR) in a study of the spin distributions produced by surrogate reactions, as well as relative $\langle\Gamma_\gamma/\Gamma_T\rangle$ as a function of spin above the neutron separation energy. This comparison utilized a new nuclear reaction code to calculate γ cascades in order to extract the spin distribution from reactions and another to calculate the spin distribution semi-classically for the (p,t) reaction. It is suggested that the spin distribution deduced for lighter Samarium nuclei may suffer from the limited applicability of extreme statistical models to spherical or lesser-studied nuclei. Further studies of nuclei in the mass region, already underway, may yield valuable information for the application of such models.

IX. ACKNOWLEDGEMENTS

This work was supported by the U.S. Department of Energy No. DE-NA0002914 and DE-NA0003780, and by Lawrence Livermore National Laboratory under Contract No. DE-AC52-07NA27344.

[1] J. D. Cramer and H. C. Britt, Phys. Rev. C **2**, 2350 (1970).
[2] N. D. Scielzo, J. E. Escher, J. M. Allmond, M. S. Basunia, C. W. Beausang, L. A. Bernstein, D. L. Bleuel, J. T. Burke, R. M. Clark, F. S. Dietrich, P. Fallon, J. Gibelin, B. L. Goldblum, S. R. Lesher, M. A. McMahan, E. B. Norman, L. Phair, E. Rodriguez-Vieitez, S. A. Sheets, I. J. Thompson, and M. Wiedeking, Phys. Rev. C **85**, 054619 (2012).
[3] J. E. Escher and F. S. Dietrich, Phys. Rev. C **81**, 024612 (2010).
[4] P. Humby, A. Simon, C. W. Beausang, J. M. Allmond, J. T. Burke, R. J. Casperson, R. Chyzh, M. Dag, K. Gell, R. O. Hughes, J. Koglin, E. McCleskey, M. McCleskey, S. Ota, T. J. Ross, A. Saastamoinen, T. Tarlow, and G. Vyas, Phys. Rev. C **94**, 064314 (2016).
[5] J. E. Escher, J. T. Burke, F. S. Dietrich, N. D. Scielzo, I. J. Thompson, and W. Younes, Rev. Mod. Phys. **84**, 353 (2012).
[6] S. Ota, J. T. Burke, R. J. Casperson, J. E. Escher, R. O. Hughes, J. J. Ressler, N. D. Scielzo, I. J. Thompson, R. A. E. Austin, B. Abromeit, N. J. Foley, E. McCleskey, M. McCleskey, H. I. Park, A. Saastamoinen, and T. J. Ross, Phys. Rev. C **92**, 054603 (2015).
[7] T. J. Ross, R. O. Hughes, J. M. Allmond, C. W. Beausang, C. T. Angell, M. S. Basunia, D. L. Bleuel, J. T. Burke, R. J. Casperson, J. E. Escher, P. Fallon, R. Hatarik, J. Munson, S. Paschalis, M. Petri, L. W. Phair, J. J. Ressler, and N. D. Scielzo, Phys. Rev. C **90**, 044323 (2014).
[8] S. R. Lesher, L. Phair, L. A. Bernstein, D. L. Bleuel, J. T. Burke, J. A. Church, P. Fallon, J. Gibelin, N. D. Scielzo, and M. Wiedeking, Nuclear Instruments and Methods in Physics Research Section A: Accelerators, Spectrometers, Detectors and Associated Equipment **621**, 286 (2010).
[9] R. O. Hughes, C. W. Beausang, T. J. Ross, J. T. Burke, R. J. Casperson, N. Cooper, J. E. Escher, K. Gell, E. Good, P. Humby, M. McCleskey, A. Saastimoinen, T. D. Tarlow, and I. J. Thompson, Phys. Rev. C **90**, 014304 (2014).
[10] R. O. Hughes, J. T. Burke, R. J. Casperson, S. Ota, S. Fisher, J. Parker, C. W. Beausang, M. Dag, P. Humby, J. Koglin, E. McCleskey, A. B. McIntosh, A. Saastamoinen, A. S. Tamashiro, E. Wilson, and T. C. Wu, Nuclear Instruments and Methods in Physics Research Section A: Accelerators, Spectrometers, Detectors and Associated Equipment **856**, 47 (2017).
[11] C. E. Porter and R. G. Thomas, Phys. Rev. **104**, 483 (1956).
[12] O. Bohigas and H. A. Weidenmuller, Annual Review of Nuclear and Particle Science **38**, 421 (1988).
[13] F. Bečvář, Nucl. Instrum. Methods A **417**, 434 (1998).
[14] N. M. Cooper, Ph.D. thesis, Yale University (2015).
[15] G. Rusev, M. Jandel, M. Krtička, C. W. Arnold, T. A. Bredeweg, A. Couture, W. A. Moody, S. M. Mosby, and J. L. Ullmann, Phys. Rev. C **88**, 057602 (2013).
[16] T. v. Egidy and D. Bucurescu, Phys. Rev. C **72**, 044311 (2005).

[17] T. von Egidy and D. Bucurescu, Phys. Rev. C **73**, 049901 (2006).
[18] R. Capote, M. Herman, P. Obloinsk, P. Young, S. Goriely, T. Belgya, A. Ignatyuk, A. Koning, S. Hilaire, V. Plujko, M. Avrigeanu, O. Bersillon, M. Chadwick, T. Fukahori, Z. Ge, Y. Han, S. Kailas, J. Kopecky, V. Maslov, G. Reffo, M. Sin, E. Soukhovitskii, and P. Talou, Nuclear Data Sheets **110**, 3107 (2009), special Issue on Nuclear Reaction Data.
[19] S. Raman, C. W. Nestor, and P. Tikkanen, Atomic Data and Nuclear Data Tables **78**, 1 (2001).
[20] M. Guttormsen, T. Tveter, L. Bergholt, F. Ingebretsen, and J. Rekstad, Nuclear Instruments and Methods in Physics Research Section A: Accelerators, Spectrometers, Detectors and Associated Equipment **374**, 371 (1996).